The effect of marrow secretome and culture environment on the rate of metastatic breast cancer cell migration in two and three dimensions

Kimberly J. Curtis[a,b], Christine Mai[c], Hannah Martin[c], Alyssa G. Oberman[a,b], Laura Alderfer[a,b], Ricardo Romero-Moreno[b,d], Mark Walsh[e,f], Stephen F. Mitros[f], Scott G. Thomas[e], Joseph A. Dynako[e], David I. Zimmer[e], Laoise M. McNamara[g], Laurie E. Littlepage[b,d], and Glen L. Niebur[a,b,c,*]

[a]Bioengineering Graduate Program; [c]Department of Aerospace and Mechanical Engineering; [d]Department of Chemistry and Biochemistry, and [b]Harper Cancer Research Institute, University of Notre Dame, IN 46556; [e]Indiana University School of Medicine, South Bend Campus, Notre Dame, IN 46556; [f]Beacon Medical Group, Trauma and Surgical Services, South Bend, IN, 46601; [g]Mechanobiology and Medical Devices Research Group, Biomedical Engineering, College of Engineering and Informatics, National University of Ireland, Galway, Ireland H91 CF50

ABSTRACT **Metastasis is responsible for over 90% of cancer-related deaths, and bone is the most common site for breast cancer metastasis. Metastatic breast cancer cells home to trabecular bone, which contains hematopoietic and stromal lineage cells in the marrow. As such, it is crucial to understand whether bone or marrow cells enhance breast cancer cell migration toward the tissue. To this end, we quantified the migration of MDA-MB-231 cells toward human bone in two- and three-dimensional (3D) environments. First, we found that the cancer cells cultured on tissue culture plastic migrated toward intact trabecular bone explants at a higher rate than toward marrow-deficient bone or devitalized bone. Leptin was more abundant in conditioned media from the cocultures with intact explants, while higher levels of IL-1β, IL-6, and TNFα were detected in cultures with both intact bone and cancer cells. We further verified that the cancer cells migrated into bone marrow using a bioreactor culture system. Finally, we studied migration toward bone in 3D gelatin. Migration speed did not depend on stiffness of this homogeneous gel, but many more dendritic-shaped cancer cells oriented and migrated toward bone in stiffer gels than softer gels, suggesting a coupling between matrix mechanics and chemotactic signals.**

Monitoring Editor
Dennis Discher
University of Pennsylvania

Received: Dec 11, 2019
Revised: Jan 21, 2021
Accepted: Mar 3, 2021

INTRODUCTION

Breast cancer metastasis commonly targets the skeleton, with over 70% of breast cancer patients having bone metastases at death (Kennecke *et al.*, 2010; Li *et al.*, 2012). Although screening methods and adjuvant therapy have reduced death rates from breast cancer in the United States by 24% (Berry *et al.*, 2005), methods of treating and preventing bone metastasis have advanced more slowly. Patients diagnosed with breast cancer metastasized to bone have a median survival of 1.6 years (Liede *et al.*, 2016). Early detection of bone metastasis is difficult, as radiography can only detect bone lesions at advanced stages of the disease after severe bone destruction due to the opaque nature of bone (Eustace *et al.*, 1997; Gauvain *et al.*, 2005). Treatments for bone metastasis include radiation, chemotherapy, and surgery (Solomayer *et al.*, 2000; Coleman, 2004). However, some patients do not respond to treatment, and recurrence is common (Cameron *et al.*, 2017; Croker *et al.*, 2017). Metastasized cancer cells also interact with resident bone cells, including primary bone cells—osteoblasts, osteoclasts, and osteocytes—to disrupt the normal mechanobiological control program, resulting in abnormal bone resorption and formation, which often causes osteolysis and increased fracture risk (Mundy, 2002;

This article was published online ahead of print in MBoC in Press (http://www.molbiolcell.org/cgi/doi/10.1091/mbc.E19-12-0682) on March 10, 2021.

*Address correspondence to: Glen L. Niebur (gniebur@nd.edu).

Abbreviations used: AB/AM, antibiotic/antimycotic; FBS, fetal bovine serum; FGF-23, fibroblast growth factor 23; H&E, hematoxylin and eosin; MSC, mesenchymal stem cell; mTGase, microbial transglutaminase; PBS, phosphate-buffered saline; PFA, paraformaldehyde; THA, total hip arthroplasty.

Coleman *et al.*, 2010). Hence, understanding the mechanisms that direct metastasis to bone will be critical to identifying potential therapeutic targets that will result in prevention or remission of metastases and the associated skeletal-related events.

Bone metastases primarily affect the axial skeleton where hematopoietic marrow is abundant (Coleman, 2006). The marrow cells are believed to express chemoattractant molecules that recruit the cancer cells and provide a suitable niche for survival (Paget, 1889; Coughlin *et al.*, 2016a). Immune cells, which make up approximately 40% of bone marrow (Zhao *et al.*, 2012, Curtis *et al.*, 2020a), mediate tumor metastasis through inflammatory responses (Balkwill *et al.*, 2005; DeNardo *et al.*, 2008). At the same time, hematopoietic precursor cells in bone marrow prepare metastatic niches for tumor cell arrival (Kaplan *et al.*, 2005), while blocking these cells inhibits tumor growth and angiogenesis (Lyden *et al.*, 2001). Adipocytes, which are a major component of bone marrow (Scheller *et al.*, 2014, Curtis *et al.*, 2020a), lose their lipid content, become fibroblastic, and increase the invasiveness of tumor cells when cocultured with tumor cells (Dirat *et al.*, 2011; Bochet *et al.*, 2013; Herroon *et al.*, 2013; Nieman *et al.*, 2013). Mesenchymal stem cells (MSCs) in the bone marrow's central sinus also interact with breast cancer cells to support tumor proliferation by releasing supportive growth factors and adhesion molecules that promote cancer cell survival (Karnoub *et al.*, 2007; Patel *et al.*, 2010; Chaturvedi *et al.*, 2014). Additionally, MSCs attract macrophages and regulatory T cells to the tumor, increasing tumor angiogenesis and decreasing the ability of the cancer cells to be recognized by the host's immune system (Patel *et al.*, 2010; Chaturvedi *et al.*, 2014).

It is crucial to understand how breast cancer cells migrate toward bone in a three-dimensional (3D) environment to mimic physiological conditions. Metastatic progression is accompanied by changes in the mechanical environment (Kumar and Weaver, 2009), and cancer cells that engraft in bone face a distinct environment with soft marrow interspersed between rigid bone struts (Curtis *et al.*, 2020a). Substrate stiffness directly impacts cancer cell proliferation and migration in 2D cell cultures. For example, breast cancer cell migration and proliferation increase with either increased stiffness of polyacrylamide gels (Tilghman *et al.*, 2010) or increased substrate degradation and traction stresses (Jerrell and Parekh, 2014). However, cancer cells in vivo must degrade and migrate through unique 3D environments of varying stiffness as they invade tissue. Breast cancer cells invade methacrylated gelatin ranging from 300 to 750 Pa (Peela *et al.*, 2016). However, it is unknown how chemoattractant factors from bone marrow affect cancer cell migration in 3D.

We recently developed a culture system to study bone colonization by growing bone and cancer cells in culture. We identified a panel of chemokines, cytokines, and growth factors that are secreted from bones cultured with cancer cells (Romero-Moreno *et al.*, 2019). Further analysis of Cxcl5, a chemokine identified by the study, identified Cxcl5 as sufficient to promote bone colonization of breast cancer cells, while inhibition of Cxcr2, the Cxcl5 receptor, was sufficient to inhibit colonization.

Understanding the factors that enhance migration of cancer cells to a particular niche can provide additional insight into how cancer cells select and colonize within a particular bone marrow niche. The objective of this study was to examine breast cancer cell migration toward bone in a 3D environment. First, the relative contributions of marrow cells versus osteocytes residing in the mineralized matrix to breast cancer chemotaxis were quantified in 2D. A panel of proteins found in bone and marrow were quantified in the media to identify potential chemoattractants. Second, breast cancer cell migration into human bone marrow was investigated in an in situ culture system. Finally, the bone marrow chemotaxis model was used to quantify the effects of scaffold stiffness on 3D breast cancer cell migration.

RESULTS AND DISCUSSION

2D cell migration toward human bone and marrow

We first studied whether the presence of bone marrow or live bone is necessary to induce breast cancer cell migration. To do this, we developed a bone explant culture system of human bone cocultured with human breast cancer cells that includes the heterogeneous cellular and protein components of human bone marrow, including immune cells. This system allows us to visualize and track human breast cancer cells in an intact human bone microenvironment. Human trabecular bone explants obtained from donors during total hip arthroplasty (THA) under Institutional Review Board (IRB) approval were cultured at the center of a colony of MDA-MB-231 cells in a 12-well plate (Figure 1A). We seeded MDA-MB-231 (triple negative breast cancer) cells in an annulus to observe migration toward the center of a 12-well culture plate. We affixed a 10-mm diameter circular magnet to the center of each well of a 12-well cell culture plate to prevent cell attachment (Figure 1A). After allowing the cells to attach for 16 h, the magnets were removed, and the cylindrical human bone explants were placed at the center of the annulus.

To delineate the role of bone marrow, osteocytes, and bone extra cellular matrix on cancer cell migration, three groups of bone explants were prepared. The first group was intact, a second group had the marrow removed by centrifugation, and the third was devitalized by repeated freeze–thaw cycles. A final group contained no bone and served as a control. Following the experiment, we verified the presence or absence of marrow with hematoxylin and eosin (H&E) histology in representative samples (Figure 1B). The marrow was successfully removed from the explants that were centrifuged (Figure 1C). Similarly, the explants that underwent repeated freeze–thaw cycles did not have osteocytes with intact nuclei in the lacunae (Figure 1D), verifying that the explants were effectively devitalized.

To determine how breast cancer cell chemotaxis was influenced by marrow cells and osteocytes residing in the mineralized matrix, we measured the migration rates of the MDA-MB-231 cells toward the human trabecular bone explants in culture by time-lapse microscopy for 24 h (Figure 1E). We chose to use the rate of cell migration as a quantitative measure of the strength of the chemoattractant signal. We used an in vitro assay to achieve greater repeatability and more precise measurements of migration rate. We did not track migration of human breast cancer cells in an animal model because we wanted to test the migration in the presence of human tissue and cytokines, which may be specific to the human cancer cell line that we studied.

The cell migration rate was highest in wells containing intact bone explants at all time points ($p < 0.05$) except 20 h when it was similar to bone without marrow (Figure 1, E and F). The migration rate was higher in wells containing bone without marrow than in wells with devitalized bone at all time points after 4 h ($p < 0.004$). The cells migrated toward the devitalized explants even more slowly than toward the empty tissue culture plastic for time periods less than 8 h ($p < 0.05$; Figure 1F) and at a similar rate thereafter.

We verified that the movement of the boundary of the cell colony was due to migration rather than proliferation. Breast cancer cell number was measured before and following the 24 h coculture with bone explants using a metabolic assay (CellTiter-Blue, Promega). The number of cancer cells in culture was similar whether the culture well contained intact bone, bone without marrow, or no bone

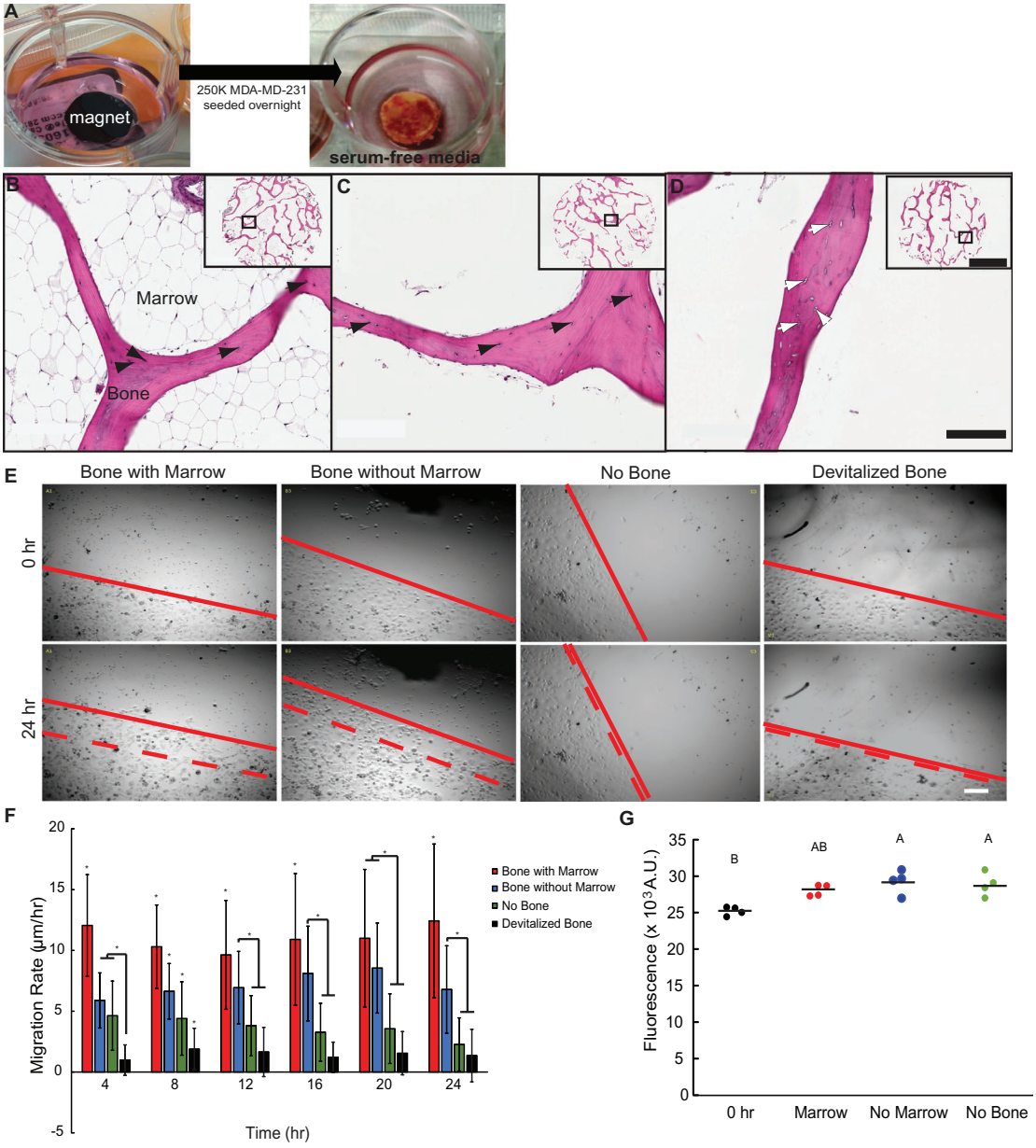

FIGURE 1: (A) Experimental setup. MDA-MB-231 cells were seeded into 12-well plates 16 h before adding the bone to the cultures. A magnet was affixed in the center of each well to prevent cell attachment. After 16 h, the magnets were replaced with bone explants and grown in serum-free media. Cylindrical trabecular bone explants were collected from femoral head tissue samples harvested from six patients undergoing THA. Representative H&E images of human bone explants with marrow (B), without marrow (C), and devitalized bone (D). Explants were fixed and stained after culture with cancer cells. Viable osteocytes are labeled with black arrows. White arrows highlight empty osteocyte lacunae that are missing nuclei. Scale bar is 200 μm in outset and 3 mm in the inset. (E) Representative images of cancer cell boundary at 0 and 24 h when cultured with different conditions of bone. Images were enhanced for visualization. Solid line indicates cell boundary; dashed line indicates initial cell boundary. Scale bar is 100 μm. (F) Migration rate of MDA-MB-231 cells at 4-h intervals over 24 h when cultured with bone with marrow, bone without marrow, no bone, or devitalized bone. The migration rate was highest when cultured with bone with marrow at every time point ($p < 0.04$) except at 20 h ($p = 0.08$ vs. live bone). The migration rate remained nearly constant over 24 h for cancer cells cultured with bone with marrow, without marrow, or devitalized bone ($p > 0.12$) but decreased over time when no bone was present ($p < 0.001$). Each condition had six biological replicates except devitalized bone ($N = 4$), and each biological replicate included four technical replicates. ANOVA was used to compare migration rates between groups at each time point (*$p < 0.05$). (G) Cell proliferation was observed when cancer cells were cultured with bone with marrow, bone without marrow, or no bone based on a CellTiter-Blue assay. The 0 h condition represents the metabolism of the cancer cells immediately prior to the addition of bone explants to the culture. Cell number increased when cancer cells were cultured with bone without marrow or no bone compared with 0 h (ANOVA; $p < 0.01$). However, the cell number was similar when MDA-MB-231 cells were cultured with bone with marrow, without marrow, or no bone, indicating that there was a similar number of cancer cells in all experimental conditions and that differences in migration were not driven by proliferation of the cancer cells (ANOVA; $p > 0.14$). See Supplemental Video S1.

($p > 0.14$; Figure 1G), indicating that the presence of the bone explants did not enhance cell proliferation in the 24 h culture period. As such, we concluded that the higher migration rate was not due to cells proliferating at the edge of the colony or migrating to provide space for new cells.

These results suggest that both bone marrow cells and osteocytes express chemokines that enhance cancer cell migration. This agrees with previous studies that found that intact trabecular bone fragments enhanced directed migration of MDA-MB-231 cells (Contag *et al.*, 2014; Templeton *et al.*, 2015), and that intact fragments increased proliferation of MDA-MB-231 cells compared with marrow-depleted bone (Contag *et al.*, 2014; Templeton *et al.*, 2015). In our experiment, we specifically showed that the presence of the marrow increases the migration rate, indicating that marrow cells release chemokines related to migration. Interestingly, we found that bone without marrow also affected cancer cell migration, suggesting a role for osteocytes, as osteocytes would make up the majority of viable cells even if some marrow cells or their remnants remained. The increasing migration rate over time is consistent with chemokines expressed by osteocytes traversing through the mineralized matrix to reach the cell culture media. These results complement an earlier study where conditioned media from osteocytes increased both proliferation and migration of MDA-MB-231 cells in 2D (Cui *et al.*, 2016). Growth factors released from the mineralized matrix, such as TGF-β and IGF-1, have been associated with tumor progression and may also influence breast cancer cell migration (Yoneda and Hiraga, 2005). However, these growth factors are sequestered in the matrix and are normally only released during bone remodeling or in acidic solutions (Pfeilschifter *et al.*, 1995). This is consistent with the failure of the devitalized bone to enhance the migration of the MDA cells in our experiment.

Inhibitory factors released by dying cells during the devitalization of the bone may explain the slightly lower migration rate measured relative to no bone. These factors may have defused or degraded over the first 8 h of culture, as there was no effect at later time points. We did not explore this because we were focused on positive regulators of migration in order to provide insight into which niche within the marrow was targeted by cancer cells.

Cytokine and chemokine analysis. Given the enhanced migration, we sought to identify cytokines and chemokines that might have affected cell migration. To analyze bone remodeling-related proteins that might affect both cancer cell migration and bone balance, we analyzed the protein content of the conditioned media from our cultures using a Human Bone 13-Plex assay performed by Eve Technologies (Supplemental Table S1). The cohort of proteins and hormones assayed was associated with bone remodeling (Supplemental Table S2). The conditioned media from cocultures of the MDA-MB-231 cells with 1) intact human trabecular bone, 2) human trabecular bone with marrow removed, or 3) with no bone were assayed. The devitalized bone-conditioned media was not assayed because the migration assays suggested that devitalized bone did not enhance cancer cell migration (Figure 1). To identify cross-talk, we also assayed conditioned media for each case with no cancer cells present, including media from empty culture wells. Leptin, IL-1β, IL-6, and TNFα concentrations were higher in cases where bone marrow was present compared with cases without bone marrow ($p < 0.05$; Figure 2A). Conditioned media from cocultures with cancer cells exhibited higher expression of DKK-1, IL-1β, IL-6, OPG, and TNFα but decreased OC expression compared with conditioned media from samples without cancer cells ($p < 0.05$; Figure 2A). Interestingly, higher levels of IL-1β, IL-6, and TNFα were found when both bone marrow and cancer cells were present ($p < 0.05$). Conditioned media from cancer cells cultured without bone explants contained elevated levels of DKK-1, OPG, and PTH compared with fresh media (Figure 2B). Levels of insulin and fibroblast growth factor 23 (FGF-23) were undetectable in any of our cultures. The latter result was unexpected, as FGF-23 is produced by osteocytes and marrow stromal cells.

Leptin was the only protein with significantly elevated levels in conditioned media from bone with marrow compared with bone without marrow regardless of the presence of the MDA-MB-231 cells. This suggests that leptin expression by adipocytes in the marrow may have increased the rate of breast cancer cell migration toward bone. The presence of leptin enhances MDA-MB-231 migration (Juárez-Cruz *et al.* 2019; Duan *et al.* 2020). To demonstrate the chemoattractant potential of leptin, we used Transwell invasion assays to quantify MDA-MB-231 migration across a Matrigel boundary. We used leptin, TNFα, and IL-1β at concentrations 10× those measured in the conditioned media in the migration experiment. We found that only leptin enhanced invasion and migration. More cells migrated toward leptin-treated media ($p < 0.01$) than control, serum-free media (Figure 3A). Migration toward TNFα and IL-1β media was similar to leptin, but not significantly greater than controls. To quantify the cross-talk, we compared migration toward media containing both TNFα and IL1- β to that containing all three cytokines. Leptin again enhanced migration ($p < 0.001$; Figure 3B). Breast cancer cell migration has previously been reported to be associated with higher levels of leptin and IL-1β in the media (Templeton *et al.*, 2015). However, other factors and cross-talk between the cell types could also be present in bone. For example, leptin enhances the migration and invasion potential of breast cancer cells and glioma cells through IL-8 expression by tumor-associated macrophages and MMP-13 production, respectively (Yeh *et al.*, 2009; Li *et al.*, 2016). Most significantly, it was recently shown that leptin enhances breast cancer cell chemotaxis through Src and FAK activation (Juárez-Cruz *et al.* 2019) and migration through the SDF-1/CXCR4 axis (Duan *et al.* 2020). Notably, we detected enhanced migration with leptin concentrations of only 5 ng/ml, compared with 100 (Juárez-Cruz *et al.* 2019) or 200 ng/ml (Duan *et al.* 2020) used in previous studies, suggesting that leptin is a more potent regulator of chemotaxis and migration than previously thought. Knockout or knockin animal models could provide more clarity regarding the role of leptin in metastasis. For example, leptin knockout rats exhibit higher bone mass compared with wild-type controls and may be a useful model to link obesity, diabetes, bone metabolism, and bone metastasis (Vaira *et al.*, 2012).

Other cytokines detected in the conditioned media have also been associated with metastatic progression. IL-1β is secreted by adipocytes and immune cells and is associated with cancer cells homing to bone (Nutter *et al.*, 2014; Templeton *et al.*, 2015). IL-6 and TNFα levels were also slightly elevated in media containing intact bone samples without cancer cells. Like IL-1β, IL-6 and TNFα are inflammatory proteins produced by bone marrow cells that are known to enhance cancer metastasis. For example, IL-6 increases breast cancer aggressiveness (Dirat *et al.*, 2011; Won *et al.*, 2013), while TNFα stimulates the production of IL-6 in MDA-MB-231 cells (Suarez-Cuervo *et al.*, 2003). In contrast, the inhibition of TNFα reduced bone metastases in vivo (Hamaguchi *et al.*, 2011). The levels of IL-1β, IL-6, and TNFα increased significantly in the presence of cancer cells, suggesting that their expression was an inflammatory response by the marrow cells through cross-talk between bone and cancer cells. IL-6 and TNFα could also play a role in aberrant bone remodeling as they enhance RANKL expression by osteoblasts in

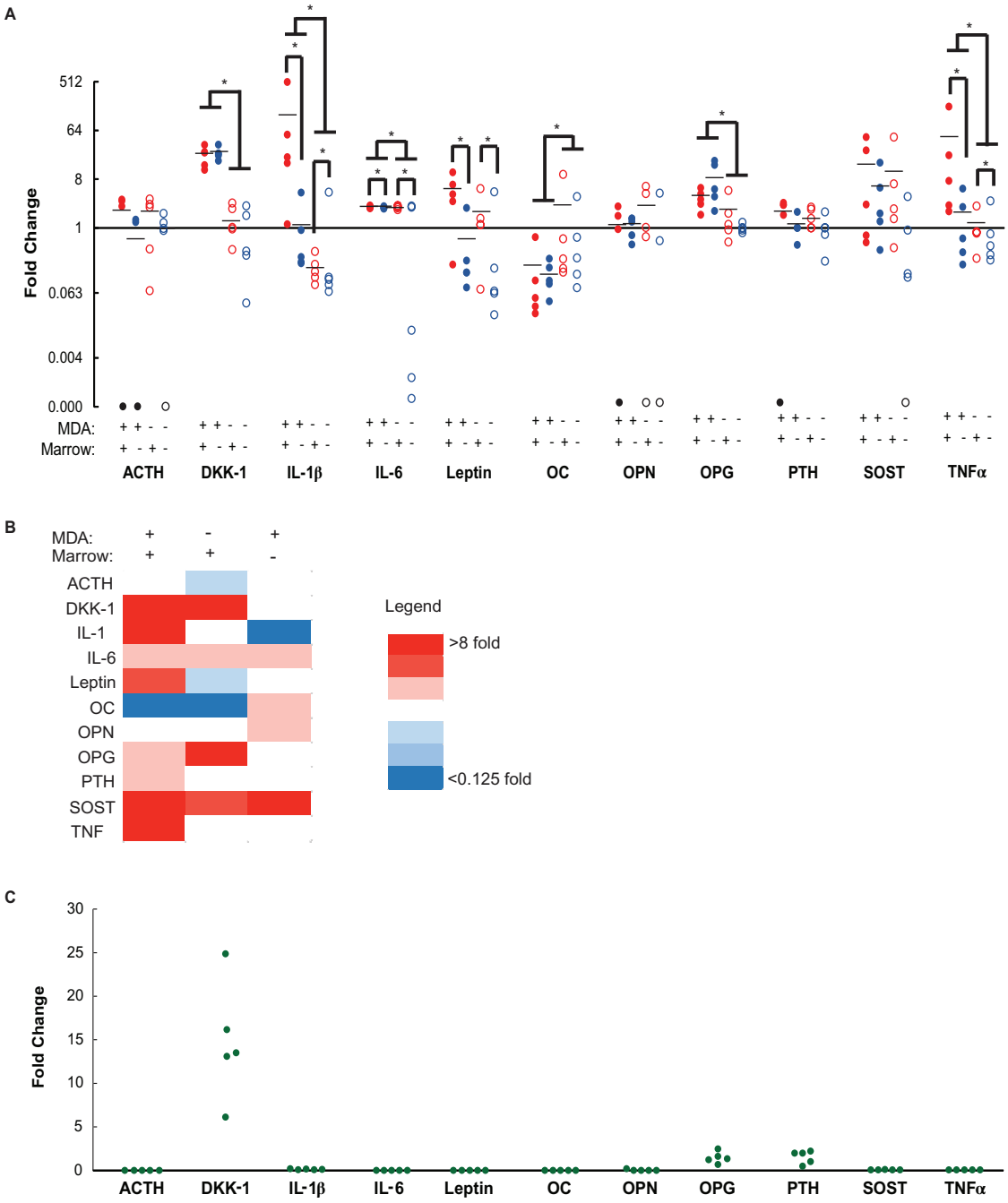

FIGURE 2: (A) Log_2 (fold-change) of protein levels in media from cultures containing human bone with (red circles) or without (blue circles) marrow and with (solid circles) or without (empty circles) cancer cells relative to the bone only with no marrow and no cancer cell case (as such, all proteins for the no marrow and no cancer cell have a mean value of 1.0). Black circles indicate one or more points at zero expression. Statistical analysis was carried out on log-transformed data to account for nonnormal distributions. Expression of IL-1β, IL-6, leptin, and TNFα were increased by the presence of marrow (*$p < 0.05$; repeated measures two-factor ANOVA). The presence of cancer cells increased expression of DKK-1, IL-1β, IL-6, OPG, and TNFα, and decreased OPN expression (*$p < 0.05$; repeated measures two-factor ANOVA). Interactions between the presence of marrow and cancer cells were observed in IL-1β and IL-6 expression. (B) The heatmap shows fold-change of expression relative to the mean of the no-marrow no-cancer cell condtions. (C) For reference, protein expression from the media of cancer cells cultured alone normalized to the no marrow no cell condition.

vivo (Wu *et al.*, 2017; Luo *et al.*, 2018). DKK-1 is also an important regulator of the WNT pathway in bone. In our cocultures, it was most highly expressed by the cancer cells. Since, DKK-1 affects the Wnt pathway to promote adipogenesis and inhibit osteogenesis of MSCs in bone marrow (Christodoulides *et al.*, 2006), this may contribute to a positive feedback loop that enhances homing of cancer cells to bone. High levels of DKK-1 expression by the MDA-MB-231 cell line are consistent with earlier reports (Templeton *et al.*, 2015). The relative number of MDA cells in the culture model in comparison to osteocytes is likely a factor in this finding as well.

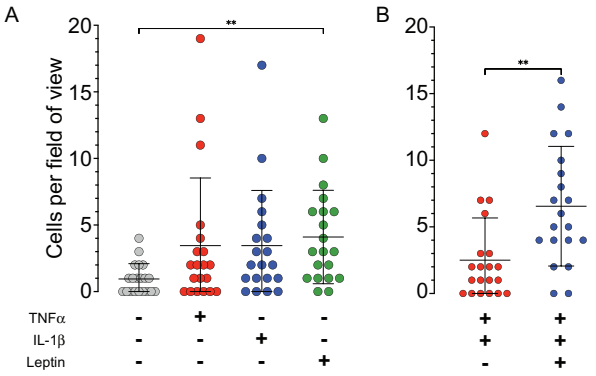

FIGURE 3: Transwell invasion assays were used to determine whether upregulated chemokines increased invasiveness of MDA-MB-231 cells. When chemokines were added individually (A), leptin increased invasion compared with controls (**$p < 0.01$). When the chambers contained combinations of chemokines (B), adding leptin to TNFα and IL-1β increased invasiveness (**$p < 0.01$).

3D migration in human bone using bioreactor culture. We next sought to determine whether the MDA-MB-231 cells would migrate through bone marrow. Cells were seeded on the top surface of human trabecular bone explants, which were subsequently cultured in an in situ bioreactor for 4 wk (Birmingham *et al.*, 2014; Coughlin *et al.*, 2016b; Curtis *et al.*, 2019, 2018). Cancer cells that have extravasated into the marrow may subsequently migrate to a preferred niche, become dormant, die, or proliferate. Our goal was to observe whether the cancer cells would migrate within the marrow. We verified that the cancer cells migrated into the bone marrow using immunohistochemistry for pan-cytokeratin (Figure 4). We imaged serial sections of the explants starting from the seeded surface and counted the percentage of positively stained cells within each section. A majority of the breast cancer cells observed were detected within 300 μm of the surface where they were initially seeded, with progressively few cells observed on sections from deeper than 300 μm in the explant (Figure 4C). We did not immunostain for specific cell surface markers that could identify individual cell types in the marrow that the cancer cells were in close proximity to. However,

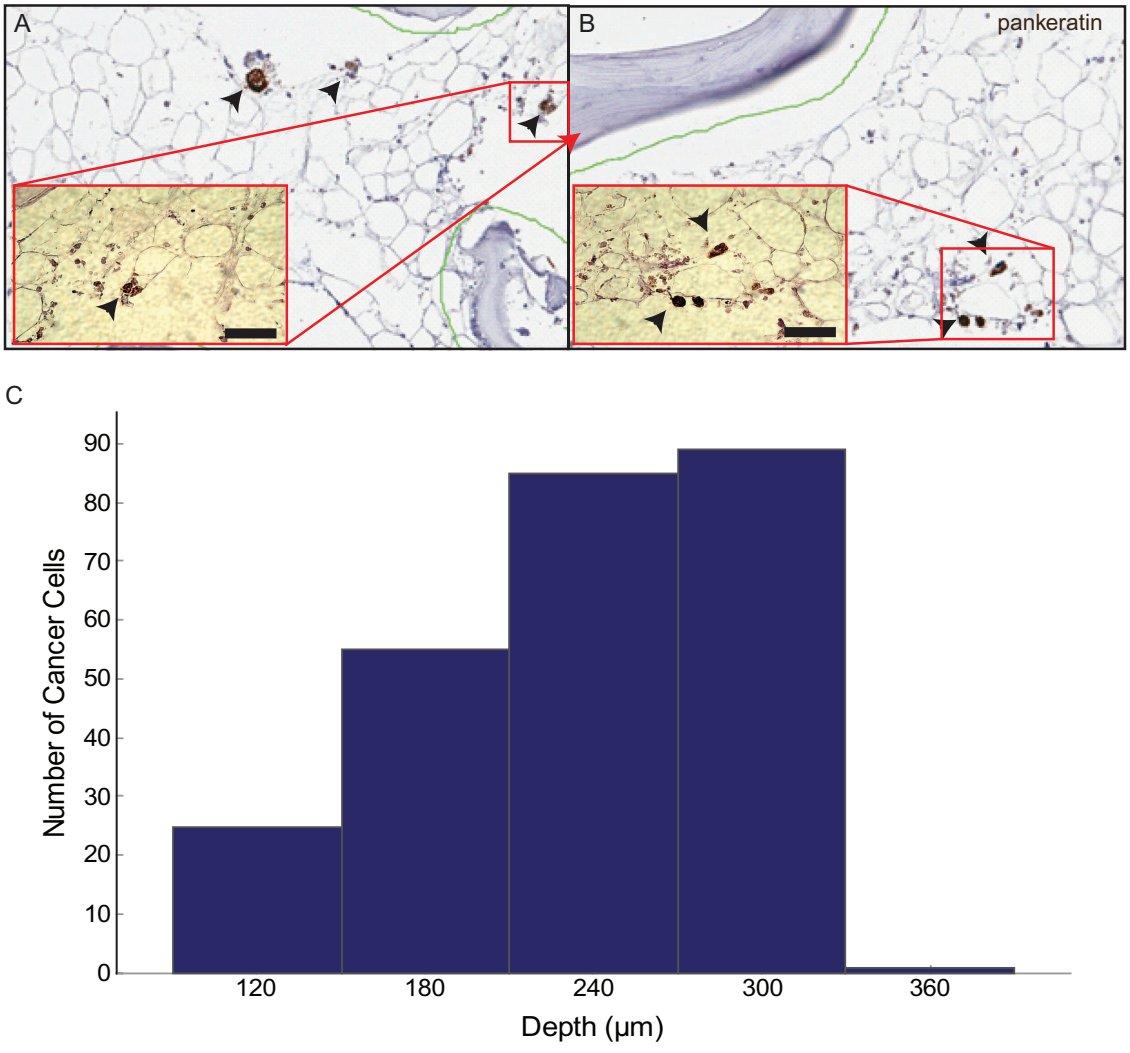

FIGURE 4: Representative images of pan keratin stained MDA-MB-231 cells (arrowheads) at depths of 200 μm (A) and 315 μm (B) from the surface of human trabecular bone explants where cells were initially seeded, indicating their migration into the bone. Scale bar is 50 μm. (C) Histogram of the number of MDA-MB-231 cells detected at various distances from the initial surface where they were seeded in seven human trabecular bone explants.

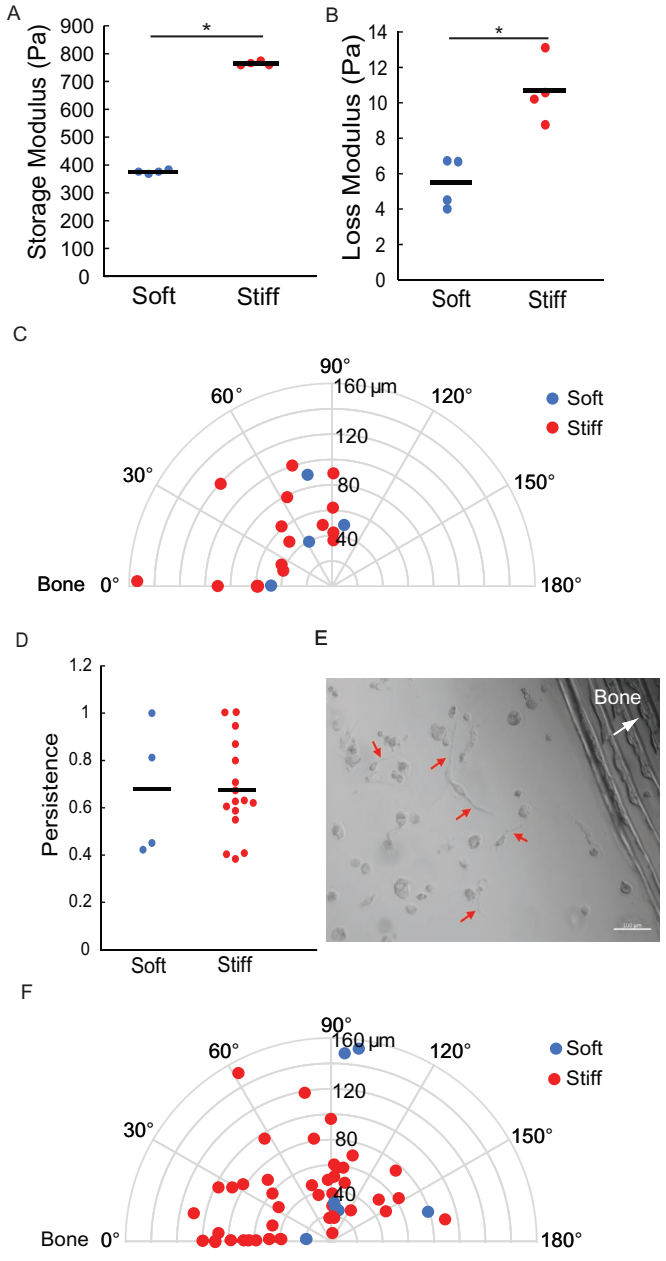

FIGURE 5: Both the storage (A) and the loss (B) moduli were nearly two times higher in gelatin hydrogels cross-linked with 0.8% mTGase per gram gelatin compared with hydrogels cross-linked with 0.3% mTGase per gram gelatin ($N = 4$; $*p = 0.001$ and $*p = 0.004$, respectively). The properties were measured at 1 Hz sinusoidal loading to 5% shear strain at the sample surface. (C) Direction and distance of migrating cells found in soft (blue) and stiff (red) hydrogels. Four percent of cells migrated in the stiff hydrogels (red) which was not significantly different than the 2.5% that migrated in soft hydrogels (blue) ($p = 0.33$; chi-squared test, $N > 200$ cells observed). The distance migrated was not dependent on the relative direction of the human bone explant containing marrow. All but one cell migrated toward or tangentially to the bone explant. (D) Persistence of breast cancer cell migration did not differ between those embedded in stiff hydrogels compared with soft hydrogels ($p = 0.97$). (E) Red arrows indicate dendritic processes formed by cancer cells cultured in stiff hydrogels at 24 h of culture. Scale bar is 100 µm. (F) Direction and length of dendritic processes found in cells embedded in soft and stiff hydrogels. Eleven percent of cells formed dendritic processes in stiff hydrogels (red) compared with 4% in soft hydrogels (blue) ($p = 0.01$; chi-squared test). A majority of the dendrites formed were directed toward the human bone explant (90° or less). See Supplemental Video S2.

most of the human marrow in these explants was comprised of adipocytes, and we found most of the cancer cells near adipocytes, complementing previous reports (Templeton *et al.*, 2015).

The explant culture bioreactor provided a physiologically relevant human marrow microenvironment to verify 3D migration. Based on the immunostaining of pan-cytokeratin, the majority of the detected breast cancer cells were single cells, rather than multicellular colonies. This was particularly true deeper within the bone explant. The detected breast cancer cells localized to the trabecular pore space surrounded by marrow. In fact, few cancer cells resided along the bone surface, suggesting that the marrow microenvironment rather than the more rigid bone is the preferred niche for the cells.

Our goal was to determine whether the MDA-MB-231 cells seeded on the marrow would migrate within the marrow, rather than simply proliferate or become dormant at the location where they were seeded. As such, we sought to model the behavior of cells after extravasation during the early stages of colonization, without the events prior to extravasation that might also impact the results and interpretation of the data. These results are consistent with our migration experiments that indicated that marrow cells provide a stronger chemoattractant environment than the bone cells. Although cancer cells migrate more readily on stiff substrates compared with soft substrates in 2D (Tilghman *et al.*, 2010; Lin *et al.*, 2016), our cancer cells readily migrated within the soft marrow in 3D. The same line of cancer cells was found to migrate readily through porous collagen scaffolds, with a bimodal dependence on the scaffold stiffness and pore size (Lang *et al.* 2015). The cancer cells may be influenced more by marrow biochemical factors or integrin and cadherin binding sites in the marrow than by the local stiffness. Several cell types, such as adipocytes, MSCs, or hematopoietic cells, and chemokines, such as SDF-1, IL-1β, and leptin, within bone marrow may recruit the cancer cells (Müller *et al.*, 2001; Kaplan *et al.*, 2005; Karnoub *et al.*, 2007; DeNardo *et al.*, 2008; Templeton *et al.*, 2015).

Cell migration toward human bone in 3D coculture. Given that the MDA-MB-231 cells migrated through the 3D bone marrow environment, we sought to determine whether chemoattractant gradients from the marrow also affect cancer cell migration in 3D cultures and whether the effect depends on the matrix mechanical properties as was previously found in porous scaffolds (Lang *et al.*, 2015). We first prepared gelatin hydrogels with two different stiffnesses that were in the range reported for bone marrow by cross-linking them with 0.3 or 0.8% microbial transglutaminase (mTGase) per gram of gelatin. Increasing the mTGase concentration increased the average shear storage modulus from 376.3 to 764.9 Pa ($p < 0.001$; Figure 5A). The loss modulus of the stiff hydrogels was also higher than that of the soft hydrogels ($p = 0.004$; Figure 5B).

We prepared 3D constructs by seeding MDA-MB-231 cells in the hydrogels surrounding a human trabecular bone explant with marrow in situ, and quantified the migration of the cancer cells using time-lapse microscopy. For each gel stiffness, approximately 200 cells were monitored for migration and formation of processes. Cells migrated toward the bone explants, with 4.2% of cells in stiff hydrogels and 2.5% of the cells embedded in soft hydrogels

migrating ($p = 0.33$; Figure 5C). On average, the cells that migrated had a net speed of 60 μm/d (total distance divided by total time) and an actual speed of 84 μm/d (step distance divided by step time), regardless of the stiffness of the hydrogel ($p = 0.97$; Figure 5D and Supplemental Video S2). The average speed was about one-third of the migration rate we found on tissue culture plastic. This is likely due to the physical differences between 2D and 3D culture environments, such as the time required for cancer cells to degrade and invade the surrounding gelatin. However, migration was much faster than that detected in the bone explants, where cancer cells only migrated as far as 350 μm into the marrow after 28 d. An important difference between migration in gelatin in comparison to the bone marrow environment is that the cells in the gelatin were likely presented with a chemoattractant gradient from the bone marrow, while cells within the marrow were surrounded by cells expressing prometastatic proteins. Indeed, the cells in the gelatin preferentially migrated toward the explant (Figure 5C). Finally, the density of cells and the presence of multiple integrin and cadherin bindings within the marrow could slow the migration of cancer cells within the marrow in comparison to gelatin.

The cancer cells also formed dendritic processes in the gels, which can be precursors to cell migration (Figure 5E). Dendritic processes were defined as extrusions from the cell that measured at least 10 μm in length found on cells that did not migrate during the 24 h study. Eleven percent of the MDA-MB-231 cells formed processes in stiff hydrogels compared with only 4.4% in soft hydrogels ($p = 0.01$), and most of the dendritic processes were extended toward the explant (Figure 5F).

It has been suggested that stiff substrates trigger a malignant migratory phenotype. Consistent with this, we found that more cancer cells migrated and formed dendritic processes in stiff hydrogels than in soft hydrogels. This result complements previous studies, which found greater cancer cell spreading and migration on stiffer substrates in 2D (Tilghman *et al.*, 2010; Sunyer *et al.*, 2012). In another study, MDA-MB-231 cells in GelMA migrated from a stiff region, with a compressive modulus of 800 Pa, toward a region with a modulus of 300 Pa, suggesting that they home toward lower stiffness environments (Peela *et al.*, 2016). The hydrogels we used had higher compressive moduli of 2280 and 1120 Pa based on the assumption that they were incompressible and isotropic. It is possible that using a stiffer hydrogel increased the migration rate in our study. However, the stiffnesses of our hydrogels were comparable to that of bone marrow, which has a reported shear modulus between 200 and 300 Pa (Winer *et al.*, 2009; Shin *et al.*, 2013). Moreover, the modulus of osteoblasts, mesenchymal stromal cells, and adipose-derived stromal cells is approximately 2.6 kPA similar to the stiffer gel we used, while mature adipocytes have an average modulus of less than 0.9 kPa, which is similar to the softer gel (Darling *et al.*, 2008). Computational models have shown that these stiffness mismatches between cell types result in protection of smaller cells from mechanical stress during bone loading (Vaughan *et al.*, 2015). In 3D culture models, the properties of the surrounding matrix also alter the size and the protein expression of spheroids formed by 4T1 cancer cells (Curtis *et al.*, 2020b).

Migration in porous scaffolds fabricated from hydrogels or natural matrices could provide an additional relevant model that captures important features of the marrow environment such as vasculature and collagen or perlecan fiber structures (Curtis *et al.*, 2020a). Stiffer matrices increased MDA-MB-231 migration rates in highly porous scaffolds, but decreased migration rate when pores were smaller than 5 μm (Lang *et al.*, 2015). However, this cell line is quite aggressive and was found to adapt migration strategies to migrate through small pores or in the face of increased cell mechanical properties (Cóndor *et al.* 2019).

Since both intact and marrow-free explants enhanced cancer cell migration in 2D, both bone and marrow cells likely contributed to migration in 3D as well. We did not use a marrow-free explant in this 3D migration experiment because we primarily wanted to understand the migration behavior in 3D and the relative contributions of chemotaxis versus matrix stiffness. We observed directed cancer cell migration toward the bone explant, suggesting that chemokines diffused from the explant through the gelatin to influence cell migration.

Taken together, our results demonstrate that MDA-MB-231 cell migration is directed by chemokines expressed by cells in the bone marrow in both 2D and 3D culture. As such, the bone marrow microenvironment may provide queues that lead to cancer cell migration to prometastatic niches within the marrow and promote the early stages of colonization.

MATERIALS AND METHODS

Request a protocol through *Bio-protocol*.

2D cell migration toward human bone and marrow

Human bone preparation. Six human femoral heads were collected from patients undergoing THA for osteoarthritis at Memorial Hospital, South Bend, IN (IRB #15-04-2500). Patients with prior history of cancer were excluded. Sixteen cylindrical trabecular bone explants with in situ marrow were prepared from each femoral head by drilling with a diamond tip drill (Starlite Industries, PA) under constant irrigation. The cores were 8 mm in diameter and approximately 3 mm in height (Figure 1A; Supplemental Video S1). The bone explants were grown with or without marrow or as devitalized bone. Unprocessed bone explants contained bone marrow (bone with marrow). For bone grown without marrow, the marrow was removed from eight explants via centrifugation at 16,000 × *g* (bone without marrow) (Curtis *et al.*, 2018). Two explants from each of four femoral heads were devitalized by freezing in liquid nitrogen and thawing at room temperature at least five times (devitalized bone). All explants were stored in serum-free, high glucose DMEM containing 1% antibiotic/antimycotic (AB/AM) (100 U/ml penicillin, 0.1 mg/ml streptomycin, and 0.25 μg/ml amphotericin B; AB/AM) for no longer than 1 h before use.

Breast cancer cell migration toward human bone. Metastatic human breast cancer cells MDA-MB-231 were cultured under standard conditions (5% CO_2, 37°C) with high glucose DMEM containing 10% fetal bovine serum (FBS) and 1% AB/AM. Sixteen hours before THA surgery, the cells were detached with trypsin-EDTA (Sigma), and 250,000 cells were seeded in each well of a 12-well plate. Before seeding the cells, a 12-mm circular magnet was placed at the center of each well and held in place with another magnet below the plate to prevent cells from attaching in that region, leaving an annulus of cancer cells (Figure 1A). After 16 h, the magnet was removed, and an 8-mm diameter bone explant was placed at the center of the annulus of cells. At the same time, the media in each well was replaced with serum-free media to limit cell proliferation (Figure 1A). Four bone explants with marrow, four bone explants without marrow, and four control wells containing no bone were studied for each of six donor bones. In addition, devitalized bone explants were studied for five donors (Table 1). The cells were incubated for 24 h while the cell migration toward the bone was tracked. Three positions along the cell boundary were imaged at 100× every hour by time-lapse microscopy to visualize cell migration using a Zeiss Axio Observer.Z1

	Bone with marrow	Bone without marrow	Devitalized bone	No bone
Biological replicates	6	6	5	6
Technical replicates	4	4	4	4
Total replicates (*N*)	24	24	20	24

TABLE 1: Number of donors and sample replicates per experimental condition.

inverted microscope (Carl Zeiss, NY). Cell boundaries within the images were measured manually relative to starting position using ImageJ (National Institutes of Health [NIH]) and used to quantify the mean cell velocity per well by dividing the mean distance between successive boundaries by the elapsed time between images.

Following culture, the bone explants were demineralized, processed for paraffin embedding, stained, and analyzed to verify the presence or absence of bone marrow and osteocytes. The explants were fixed in 4% paraformaldehyde (PFA) overnight at 4°C, then rinsed in phosphate-buffered saline (PBS) and demineralized in neutral buffered 10% EDTA for 7–10 d at room temperature. The demineralized explants were then processed to dehydrate, embedded in paraffin, and sectioned at 5 µm for histological staining. Sections were stained with H&E following manufacturer's instructions (Leica) and imaged at 200× using an Aperio CT slide scanner (Aperio Technologies).

CellTiter-Blue assay for cancer cell proliferation. A metabolic assay (CellTiter-Blue, Promega) was used to measure cell numbers in order to verify that the movement of the cell boundary was due to migration rather than expansion of the colony due to proliferation. The assay was carried out following manufacturer's instructions. Briefly, at the end of the 24-h migration experiment, the bone explants were removed from the wells and the MDA-MB-231 cells were rinsed with PBS. Media containing serum and 20% CellTiter-Blue reagent was added to each well and incubated for 3 h at 37°C. After incubation, aliquots of each supernatant were transferred in triplicate to a 96-well plate, and fluorescence was measured with 570 nm excitation and 600 nm emission. The assay was also used on cells before the magnets were replaced with bone to quantify cell proliferation over time.

Conditioned media analysis. Conditioned media from each well of the 2D migration experiments containing live bone with or without marrow was aspirated and stored at –80°C until analyzed. The media was shipped on dry ice to Eve Technologies, where it was processed according to the company's specifications and requirements to measure expression levels of 13 chemokines by a human bone chemokine discovery assay (Human Bone 13-Plex, Eve Technologies, Calgary, CA). Media was analyzed from cultures containing MDA-MB-231 cells grown with explants of bone with marrow, bone without marrow, or no bone. Conditioned media from bone explants cultured without cancer cells was also analyzed to identify proteins whose expression was affected by the MDA-MB-231 cells.

Invasion assays

Matrigel invasion assays were performed following the Transwell chamber method, using 24-well plates containing inserts of 8-mm pore size (Corning, Kennebunk, ME). Briefly, 300 µg/cm^2 of Matrigel (Corning) were added into the inserts and kept at 37°C for 3 h to form a gel. Cells were plated at 50×10^3 cells per insert in serum-free medium on the top chamber. The lower chamber of the control wells ($N = 4$) contained serum-free DMEM while experimental wells contained DMEM supplemented with 5.25 ng/ml leptin (Novus Biologicals NBP2-34934), 500 pg/ml TNFα (R&D Systems 210-TA), or 1.25 ng/ml IL-1β (R&D Systems 210-LB) ($N = 4$ per condition). Cells were incubated for 24 h at 37°C in a 5% CO_2 atmosphere. Afterward, cells and Matrigel on the upper surface of the membrane were removed with cotton swabs. Cells on the lower surface of the membrane were washed and fixed with 4% PFA for 5 min and stained with 0.5% crystal violet in PBS. Five nonoverlapping regions on each membrane were imaged on a Leica DMi8 microscope at 100×, and the number of invading cells in each image was counted manually. The number of cells per field of view in each condition was compared using Kruskall–Wallace or Mann–Whitney tests.

Migration of MDA-MB-231 cells in human bone explants

Four cylindrical human trabecular bone explants were harvested from one patient undergoing THA under informed consent, as described above. The bone explants were seeded with 100,000 MDA-MB-231 cells placed in a 12-well tissue culture plate overnight containing DMEM with 10% FBS and 1% AB/AM. Media was filled to just below the top surface of the explant to enable the cancer cells to attach to the explants for 1 h before being submerged in media. The following day, the seeded bone explants were placed into a bioreactor previously described (Birmingham *et al.*, 2014; Coughlin *et al.*, 2016b; Curtis *et al.*, 2018, 2019; Breuer *et al.*, 2019). The explants were cultured for 4 wk with half of the media replaced twice per week.

Immunohistochemistry was used to identify MDA-MB-231 cells that migrated into the bone explant. Following culture, the explants were removed from the bioreactor and fixed in 4% PFA overnight at 4°C. The fixed explants were rinsed in PBS and demineralized in neutral-buffered 10% EDTA for 7–10 d at room temperature, processed, embedded in paraffin, and sectioned at 5 µm. Sections were cleared in xylene and rehydrated through decreasing concentrations of ethanol, then stained with anti-pankeratin antibody at a concentration of 1:500 (clone Ab-1 E1/AE3; Thermo). Sections were incubated with an anti-mouse HRP–conjugated polymer (Dako) and scanned by an Aperio CT slide scanner (Aperio Technologies) with a 20× objective. Image analysis of pan-cytokeratin was completed using the Aperio Cytoplasmic algorithm with customized macro parameters set to score DAB and hematoxylin chromogen intensities. The raw data generated from the cytoplasmic algorithms included the percentage of DAB positive cells, intensity of the stain, and the area of analysis. After running the customized macros, a representative markup image was generated and re-evaluated to confirm the accuracy of the algorithms (Supplemental Figure S1).

Migration toward human bone in 3D culture

Gelatin-mTGase hydrogels were prepared by mixing gelatin (type A, 175 Bloom, Sigma) in serum-free DMEM culture medium to a concentration of 6% wt/vol. The solution was heated at 80°C for 30 min, sterile-filtered through a 0.22-µm filter (Millipore), and stored at 4°C overnight. mTGase (Activa TI; containing 1% mTGase; Modernist Pantry, ME) was mixed in sterile PBS before sterile

filtration and storage at –20°C until use. Two different concentrations of mTGase (0.3 and 0.8% mTGase per gram gelatin) were used to create soft and stiff hydrogels, respectively. Gelatin solution, mTGase solution, and cell media were mixed at a 5:4:1 (v:v:v) to yield final concentrations of 3% gelatin with either 0.3 or 0.8% mTGase per gram of gelatin; 200 µl of gel mixture was pipetted into a 8-mm mold to a height of 3.5 mm and allowed to polymerize at 4°C for 20 min. Hydrogels were allowed to come to room temperature before mechanical testing. Storage and loss moduli were measured at 1 Hz sinusoidal loading to 5% shear strain at the sample surface using a Discovery Hybrid Rheometer with flat platens (TA Instruments, New Castle, DE; $N = 4$ per stiffness). A strain sweep was used to determine the maximum amplitude of the loading.

To embed cancer cells within the hydrogels, the gelatin mixture was prepared as above, except that cell media was replaced with a cell suspension containing 10^6 MDA-MB-231 cells/ml for a final cell concentration of 10^5 cells/ml. One milliliter of mixture was added to each well of a 12-well plate ($N = 6$ per stiffness) and polymerized for 20 min at 4°C. After polymerization, a sterile 8-mm biopsy punch was used to create a central cylindrical hole in the hydrogel. Twelve human trabecular bone explants containing marrow collected from one patient were prepared as described previously and placed in the hole that was punched in each hydrogel. The media in each well was replaced with serum-free media to limit cell proliferation, and the cells were incubated for 24 h while five locations near the explant/hydrogel interface were imaged at 50× every 15 min to visualize cell migration by time-lapse microscopy, as described above. For each gel stiffness, approximately 200 cells were monitored for migration. Individual cell movement was quantified using ImageJ (NIH), as was the angle of cell migration relative to the bone. In addition, the length and direction of dendritic processes emanating from cells were measured. Dendritic processes were defined as extrusions from any cell that did not exhibit nuclear movement.

Statistical analysis

Statistical analysis was performed in Minitab 17 (State College, PA). Cell migration rates at each time point and cell viability were analyzed by ANOVA. The protein array data were log-transformed and analyzed by two-factor ANOVA (± marrow and ± MDA-MB-231 cells) using repeated measures within patients to assess which chemokine and cytokine levels differed between the experimental conditions. The tendency of breast cancer cells to migrate and form dendritic processes in gelatin hydrogels was analyzed with a chi-squared association test.

ACKNOWLEDGMENTS

This work was supported in part by the Orthopaedic Research Society Collaborative Exchange Grant (K.J.C., L.M.M., and G.L.N.), the Harper Cancer Research Institute and Walther Cancer Foundation Interdisciplinary Interface Training Program (K.J.C.), the Advanced Diagnostics & Therapeutics Leiva Graduate Fellowship in Precision Medicine (K.J.C.), the Walther Cancer Foundation, Simon-Harper Inter-Institutional Research Team Grant (L.E.L. and G.L.N.), the Walther Cancer Foundation Engineering Novel Solutions to Cancer's Challenges at the Interdisciplinary Interface Training Project (R.R.M.), the Kelly Cares Foundation (L.E.L. and G.L.N), the American Cancer Society Research Scholar Award (L.E.L.), NIH R33 CA206922 (L.E.L.), the S.A.S. Foundation for Cancer Research HHS-0008-16SF (L.E.L.), and the Indiana Clinical Translational Science Institute (NIH TL1 TR002531) (L.E.L.)

REFERENCES

Balkwill F, Charles KA, Mantovani A (2005). Smoldering and polarized inflammation in the initiation and promotion of malignant disease. Cancer Cell 7, 211–217.

Berry DA, Cronin KA, Plevritis SK, Fryback DG, Clarke L, Zelen M, Mandelblatt JS, Yakovlev AY, Habbema JDF, Feuer EJ, Cancer Intervention and Surveillance Modeling Network (CISNET) Collaborators (2005). Effect of screening and adjuvant therapy on mortality from breast cancer. N Engl J Med 353, 1784–1792.

Birmingham E, Kreipke TC, Dolan EB, Coughlin TR, Owens P, McNamara LM, Niebur GL, McHugh PE (2014). Mechanical stimulation of bone marrow in situ induces bone formation in trabecular explants. Ann Biomed Eng 43, 1036–1050.

Bochet L, Lehuédé C, Dauvillier S, Wang YY, Dirat B, Laurent V, Dray C, Guiet R, Maridonneau-Parini I, Le Gonidec S, *et al.* (2013). Adipocyte-derived fibroblasts promote tumor progression and contribute to the desmoplastic reaction in breast cancer. Cancer Res 73, 5657–5668.

Breuer E-K, Fukushiro-Lopes D, Dalheim A, Burnette M, Zartman J, Kaja S, Wells C, Campo L, Curtis KJ, Romero-Moreno R, *et al.* (2019). Potassium channel activity controls breast cancer metastasis by affecting β-catenin signaling. Cell Death Dis 10, 180.

Cameron D, Piccart-Gebhart MJ, Gelber RD, Procter M, Goldhirsch A, de Azambuja E, Castro G, Untch M, Smith I, Gianni L, *et al.* (2017). 11 years' follow-up of trastuzumab after adjuvant chemotherapy in HER2-positive early breast cancer: final analysis of the HERceptin Adjuvant (HERA) trial. Lancet Lond. Engl 389, 1195–1205.

Chaturvedi P, Gilkes DM, Takano N, Semenza GL (2014). Hypoxia-inducible factor-dependent signaling between triple-negative breast cancer cells and mesenchymal stem cells promotes macrophage recruitment. Proc Natl Acad Sci USA 111, E2120–E2129.

Christodoulides C, Laudes M, Cawthorn WP, Schinner S, Soos M, O'Rahilly S, Sethi JK, Vidal-Puig A (2006). The Wnt antagonist Dickkopf-1 and its receptors are coordinately regulated during early human adipogenesis. J Cell Sci 119, 2613–2620.

Coleman RE (2006). Clinical features of metastatic bone disease and risk of skeletal morbidity. Clin Cancer Res 12, 6243s–6249s.

Coleman RE (2004). Bisphosphonates: clinical experience. The Oncologist 9, 14–27.

Coleman RE, Lipton A, Roodman GD, Guise TA, Boyce BF, Brufsky AM, Clézardin P, Croucher PI, Gralow JR, Hadji P, *et al.* (2010). Metastasis and bone loss: advancing treatment and prevention. Cancer Treat Rev 36, 615–620.

Cóndor M, Mark C, Gerum RC, Grummel NC, Bauer A, García-Aznar JM, Fabry B (2019). Breast cancer cells adapt contractile forces to overcome steric hindrance. Biophys J 116, 1305–1312.

Contag CH, Lie W-R, Bammer MC, Hardy JW, Schmidt TL, Maloney WJ, King BL (2014). Monitoring dynamic interactions between breast cancer cells and human bone tissue in a co-culture model. Mol Imaging Biol 16, 158–166.

Coughlin T, Moreno RR, Mason D, Nystrom L, Boerckel J, Niebur G, Littlepage LE (2016a). Bone: a fertile soil for cancer metastasis. Curr Drug Targets 18, 1281–1295.

Coughlin TR, Schiavi J, Alyssa Varsanik M, Voisin M, Birmingham E, Haugh MG, McNamara, LM, Niebur GL (2016b). Primary cilia expression in bone marrow in response to mechanical stimulation in explant bioreactor culture. Eur Cell Mater 32, 111–122.

Croker AK, Rodriguez-Torres M, Xia Y, Pardhan S, Leong HS, Lewis JD, Allan AL (2017). Differential functional roles of ALDH1A1 and ALDH1A3 in mediating metastatic behavior and therapy resistance of human breast cancer cells. Int J Mol Sci 18. https://doi.org/10.3390/ijms18102039

Cui Y-X, Evans BAJ, Jiang WG (2016). New roles of osteocytes in proliferation, migration and invasion of breast and prostate cancer cells. Anticancer Res 36, 1193–1201.

Curtis KJ, Coughlin TR, Mason DE, Boerckel JD, Niebur GL (2018). Bone marrow mechanotransduction in porcine explants alters kinase activation and enhances trabecular bone formation in the absence of osteocyte signaling. Bone 107, 78–87.

Curtis KJ, Coughlin TR, Varsanik MA, Niebur GL (2019). Shear stress in bone marrow has a dose dependent effect on cFos gene expression in in situ culture. Cell Mol Bioeng. https://doi.org/10.1007/s12195-019-00594-z

Curtis KJ, Oberman AG, Niebur GL (2020a). Effects of mechanobiological signaling in bone marrow on skeletal health. Ann NY Acad Sci 1460, 11–24.

Curtis KJ, Schiavi J, Garrigle MJM, Kumar V, McNamara LM, Niebur GL (2020b). Mechanical stimuli and matrix properties modulate cancer spheroid growth in three-dimensional gelatin culture. J Roy Soc Interface 17, 20200568.
Darling EM, Topel M, Zauscher S, Vail TP, Guilak F (2008). Viscoelastic properties of human mesenchymally-derived stem cells and primary osteoblasts, chondrocytes, and adipocytes. J Biomech 41, 454–464.
DeNardo DG, Johansson M, Coussens LM (2008). Immune cells as mediators of solid tumor metastasis. Cancer Metastasis Rev 27, 11–18.
Dirat B, Bochet L, Dabek M, Daviaud D, Dauvillier S, Majed B, Wang YY, Meulle A, Salles B, Le Gonidec S, *et al.* (2011). Cancer-associated adipocytes exhibit an activated phenotype and contribute to breast cancer invasion. Cancer Res 71, 2455–2465.
Duan L, Lu Y, Xie W, Nong L, Jia Y, Tan A, Liu Y (2020). Leptin promotes bone metastasis of breast cancer by activating the SDF-1/CXCR4 axis. Aging (Albany NY). 12, 16172–16182.
Eustace S, Tello R, DeCarvalho V, Carey J, Wroblicka JT, Melhem ER, Yucel EK (1997). A comparison of whole-body turboSTIR MR imaging and planar 99mTc-methylene diphosphonate scintigraphy in the examination of patients with suspected skeletal metastases. AJR Am J Roentgenol 169, 1655–1661.
Gauvain KM, Garbow JR, Song S-K, Hirbe AC, Weilbaecher K (2005). MRI detection of early bone metastases in B16 mouse melanoma models. Clin Exp Metastasis 22, 403–411.
Hamaguchi T, Wakabayashi H, Matsumine A, Sudo A, Uchida A (2011). TNF inhibitor suppresses bone metastasis in a breast cancer cell line. Biochem Biophys Res Commun 407, 525–530.
Herroon MK, Rajagurubandara E, Hardaway AL, Powell K, Turchick A, Feldmann D, Podgorski I (2013). Bone marrow adipocytes promote tumor growth in bone via FABP4-dependent mechanisms. Oncotarget 4, 2108–2123.
Juárez-Cruz J, Zuñiga-Eulogio M, Olea-Flores M, Castañeda-Saucedo E, Mendoza-Catalán M, Ortuño-Pineda C, Moreno-Godínez M, Villegas-Comonfort S, Padilla-Benavides T, Navarro-Tito N (2019). Leptin induces cell migration and invasion in a FAK-Src-dependent manner in breast cancer cells, Endocr. Connect 8, 1539–1552.
Jerrell RJ, Parekh A (2014). Cellular traction stresses mediate extracellular matrix degradation by invadopodia. Acta Biomater. 10, 1886–1896.
Kaplan RN, Riba RD, Zacharoulis S, Bramley AH, Vincent L, Costa C, MacDonald DD, Jin DK, Shido K, Kerns SA, *et al.* (2005). VEGFR1-positive haematopoietic bone marrow progenitors initiate the pre-metastatic niche. Nature 438, 820–827.
Karnoub AE, Dash AB, Vo AP, Sullivan A, Brooks MW, Bell GW, Richardson AL, Polyak K, Tubo R, Weinberg RA (2007). Mesenchymal stem cells within tumour stroma promote breast cancer metastasis. Nature 449, 557–563.
Kennecke H, Yerushalmi R, Woods R, Cheang MCU, Voduc D, Speers CH, Nielsen TO, Gelmon K (2010). Metastatic behavior of breast cancer subtypes. J Clin Oncol 28, 3271–3277.
Kumar S, Weaver VM (2009). Mechanics, malignancy, and metastasis: the force journey of a tumor cell. Cancer Metastasis Rev 28, 113–127.
Lang NR, Skodzek K, Hurst S, Mainka A, Steinwachs J, Schneider J, Aifantis KE, Fabry B (2015). Biphasic response of cell invasion to matrix stiffness in three-dimensional biopolymer networks. Acta Biomater 13, 61–67.
Li K, Wei L, Huang Y, Wu Y, Su M, Pang X, Wang N, Ji F, Zhong C, Chen T (2016). Leptin promotes breast cancer cell migration and invasion via IL-18 expression and secretion. Int. J Oncol 48, 2479–2487.
Li S, Peng Y, Weinhandl ED, Blaes AH, Cetin K, Chia VM, Stryker S, Pinzone JJ, Acquavella JF, Arneson TJ (2012). Estimated number of prevalent cases of metastatic bone disease in the US adult population. Clin Epidemiol 4, 87–93.
Liede A, Jerzak KJ, Hernandez RK, Wade SW, Sun P, Narod SA (2016). The incidence of bone metastasis after early-stage breast cancer in Canada. Breast Cancer Res Treat 156, 587–595.
Lin P-Y, Chu Y-S, Lai Y-T, Lo C-M (2016). Interplay between substrate stiffness and TGF-b1 on cellular traction force and migration of MDA-MB-231 cells. FASEB J 30, 1300.5-1300.5.
Luo G, Li F, Li X, Wang Z-G, Zhang B (2018). TNF-α and RANKL promote osteoclastogenesis by upregulating RANK via the NF-κB pathway. Mol Med Rep 17, 6605–6611.
Lyden D, Hattori K, Dias S, Costa C, Blaikie P, Butros L, Chadburn A, Heissig B, Marks W, Witte L, *et al.* (2001). Impaired recruitment of bone-marrow-derived endothelial and hematopoietic precursor cells blocks tumor angiogenesis and growth. Nat Med 7, 1194–1201.
Müller A, Homey B, Soto H, Ge N, Catron D, Buchanan ME, McClanahan T, Murphy E, Yuan W, Wagner SN, *et al.* (2001). Involvement of chemokine receptors in breast cancer metastasis. Nature 410, 50–56.
Mundy GR (2002). Metastasis: Metastasis to bone: causes, consequences and therapeutic opportunities. Nat Rev Cancer 2, 584–593.
Nieman KM, Romero IL, Van Houten B, Lengyel E (2013). Adipose tissue and adipocytes support tumorigenesis and metastasis. Biochim Biophys Acta 1831, 1533–1541.
Nutter F, Holen I, Brown HK, Cross SS, Evans CA, Walker M, Coleman RE, Westbrook JA, Selby PJ, Brown JE, Ottewell PD (2014). Different molecular profiles are associated with breast cancer cell homing compared with colonisation of bone: evidence using a novel bone-seeking cell line. Endocr Relat Cancer 21, 327–341.
Paget S (1889). The distribution of secondary growths in cancer of the breast. The Lancet, 133, 571–573.
Patel SA, Meyer JR, Greco SJ, Corcoran KE, Bryan M, Rameshwar P (2010). Mesenchymal stem cells protect breast cancer cells through regulatory T cells: role of mesenchymal stem cell-derived TGF-beta. J Immunol 184, 5885–5894.
Peela N, Sam FS, Christenson W, Truong D, Watson AW, Mouneimne G, Ros R, Nikkhah M (2016). A three dimensional micropatterned tumor model for breast cancer cell migration studies. Biomaterials 81, 72–83.
Pfeilschifter J, Laukhuf F, Müller-Beckmann B, Blum WF, Pfister T, Ziegler R (1995). Parathyroid hormone increases the concentration of insulin-like growth factor-I and transforming growth factor beta 1 in rat bone. J Clin Invest 96, 767–774.
Romero-Moreno R, Curtis KJ, Coughlin TR, Miranda-Vergara MC, Dutta S, Natarajan A, Facchine BA, Jackson KM, Nystrom L, Li J, *et al.* (2019). The CXCL5/CXCR2 axis is sufficient to promote breast cancer colonization during bone metastasis. Nat Commun 10, 4404.
Scheller EL, Troiano N, Vanhoutan JN, Bouxsein MA, Fretz JA, Xi Y, Nelson T, Katz G, Berry R, Church CD, *et al.* (2014). Use of osmium tetroxide staining with microcomputerized tomography to visualize and quantify bone marrow adipose tissue in vivo. Methods Enzymol 537, 123–139.
Shin J-W, Swift J, Ivanovska I, Spinler KR, Buxboim A, Discher DE (2013). Mechanobiology of bone marrow stem cells: from myosin-II forces to compliance of matrix and nucleus in cell forms and fates. Differ Res Biol Divers 86, 77–86.
Solomayer EF, Diel IJ, Meyberg GC, Gollan C, Bastert G (2000). Metastatic breast cancer: clinical course, prognosis and therapy related to the first site of metastasis. Breast Cancer Res Treat 59, 271–278.
Suarez-Cuervo C, Harris KW, Kallman L, Kalervo Väänänen H, Selander KS (2003). Tumor necrosis factor-α induces interleukin-6 production via extracellular-regulated kinase 1 activation in breast cancer cells. Breast Cancer Res Treat 80, 71–78.
Sunyer R, Jin AJ, Nossal R, Sackett DL (2012). Fabrication of hydrogels with steep stiffness gradients for studying cell mechanical response. PLoS One 7, e46107.
Templeton ZS, Lie W-R, Wang W, Rosenberg-Hasson Y, Alluri RV, Tamaresis JS, Bachmann MH, Lee K, Maloney WJ, Contag CH, King BL (2015). Breast cancer cell colonization of the human bone marrow adipose tissue niche. Neoplasia 17, 849–861.
Tilghman RW, Cowan CR, Mih JD, Koryakina Y, Gioeli D, Slack-Davis JK, Blackman BR, Tschumperlin DJ, Parsons JT (2010). Matrix rigidity regulates cancer cell growth and cellular phenotype. PLoS One 5. https://doi.org/10.1371/journal.pone.0012905
Vaira S, Yang C, McCoy A, Keys K, Xue S, Weinstein EJ, Novack DV, Cui X (2012). Creation and preliminary characterization of a leptin knockout rat. Endocrinology 153, 5622–5628.
Vaughan TJ, Voisin M, Niebur GL, McNamara LM (2015). Multiscale modeling of trabecular bone marrow: understanding the micromechanical environment of mesenchymal stem cells during osteoporosis. J Biomech Eng 137. https://doi.org/10.1115/1.4028986
Winer JP, Janmey PA, McCormick ME, Funaki M (2009). Bone marrow-derived human mesenchymal stem cells become quiescent on soft substrates but remain responsive to chemical or mechanical stimuli. Tissue Eng Part A 15, 147–154.
Won HS, Kim YA, Lee JS, Jeon EK, An HJ, Sun DS, Ko YH, Kim JS (2013). Soluble interleukin-6 receptor is a prognostic marker for relapse-free survival in estrogen receptor-positive breast cancer. Cancer Invest 31, 516–521.
Wu Q, Zhou X, Huang D, Ji Y, Kang F (2017). IL-6 enhances osteocyte-mediated osteoclastogenesis by promoting JAK2 and RANKL activity in vitro. Cell Physiol Biochem 41, 1360–1369.
Yeh W-L, Lu D-Y, Lee M-J, Fu W-M (2009). Leptin induces migration and invasion of glioma cells through MMP-13 production. Glia 57, 454–464.
Yoneda T, Hiraga T (2005). Crosstalk between cancer cells and bone microenvironment in bone metastasis. Biochem Biophys Res Commun 328, 679–687.
Zhao E, Xu H, Wang L, Kryczek I, Wu K, Hu Y, Wang G, Zou W (2012). Bone marrow and the control of immunity. Cell Mol Immunol 9, 11–19.